View metadata, citation and similar papers at core.ac.uk

brought to you by CORE

provided by NASA Technical Reports Server

NASA-CR-195116

IN-20-CR

3843

33P

THE UNIVERSITY OF ALABAMA IN HUNTSVILLE

SUMMER FACULTY FELLOWSHIP RESEARCH
CONTINUATION PROGRAM

NAG8-212, TASK 9
5-30175

FINAL REPORT

Submitted to:

George C. Marshall Space Flight Center
National Aeronautics and Space Administration
Marshall Space Flight Center, AL 35812

Prepared by:

Gerald R. Karr, Ph.D.
Principal Investigator
Professor and Chairman
Department of Mechanical and Aerospace Engineering
The University of Alabama in Huntsville
Huntsville, AL 35899
205/895-6154

Submitted by:

The University of Alabama in Huntsville

April, 1994

N94-29848
Unclas
G3/20 0003843

(NASA-CR-195116) ASPECTS OF MODEL-BASED ROCKET ENGINE CONDITION MONITORING AND CONTROL Final Report (Alabama Univ.) 33 p

Aspects of Model-Based Rocket Engine Condition Monitoring and Control

A Final Report Submitted to

Dr. Gerald R. Karr, Director
NASA/ASEE 1991 Summer Faculty Fellowship Program
at the Marshall Space Flight Center

Mechanical Engineering Department
The University of Alabama at Huntsville
Huntsville, Alabama 35899

by

Arthur J. Helmicki
Department of Electrical and Computer Engineering
University of Cincinnati
Cincinnati, Ohio 45221-0030

Contents

1 Introduction 2
- 1.1 Current Approaches to SSME Modeling 3
- 1.2 Control and Condition Monitoring Based Approach 4
- 1.3 Research Assistants 5

2 Summary 6

3 Overview 7

4 Nomenclature 8

5 Equation of State for LH_2 and LOX 9

6 Dynamic Fluid Flow Through a Control Volume 13

7 Nondimensionalization 15

8 Discretization 17

9 State Assignment 19

10 Forcing Terms 20

11 SSME HPFP Nominal Model 22

12 SSME HPFP Anomalous Model 26
- 12.1 Pump Speed Disturbance 26
- 12.2 Fuel Leak 27

13 Conclusions 29

References 31

1 Introduction

Modern rocket engine systems often utilize some type of control scheme in order to achieve requirements on system performance. The increased sophistication of space missions demands that rocket engine systems not only be reliable, but also have low maintenance costs and longer life spans. So, in order to enhance reliability, extend system life, and reduce operating costs the development of condition monitoring systems, which would augment the control system is currently under study. Previous investigation of the issues involved in the design of condition monitoring systems lead to a proposed the design of condition monitoring systems using a novel approach; one that viewed the condition monitoring problem and the control design problem from within a common system-theoretic framework [15, 14]. This approach was chosen because it possesses two major advantages over traditional approaches to the study of the condition monitoring problem. For one, it characterizes the extent to which trade-offs exist between control design objectives and condition monitoring objectives and moreover, it provides a way to quantify these trade-offs. Secondly, since this approach is based on existing system-theoretic concepts, the full range of system design tools can be utilized in the analysis and design of control and condition monitoring systems. In contrast, other approaches such as [24, 25, 16, 23] focus solely on the condition monitoring aspect and do not consider any possible effects on the control system. Moreover, the interaction between the condition monitoring and control systems has not been addressed.

The integrated approach to condition monitoring and control is predicated on the ability to model anomalous conditions arising in rocket engine systems. The need for rocket engine models able to predict both nominal and anomalous behavior motivated the work presented here. A modeling scheme for anomalous conditions should prove itself compatible with system analysis tools. Two such schemes are introduced here: signal representation and uncertainty representation. [13, 15, 14]. Figures 1 and 2 depict the general configuration of the two schemes. The nominal

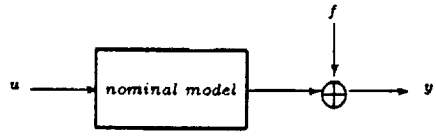

Figure 1: Signal Representation

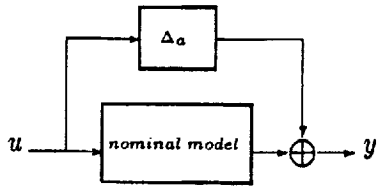

Figure 2: Uncertainty Representation

model blocks in Figures 1 and 2 can represent an entire system or just one of its components. In the case of Figure 1 anomalous conditions are represented by the injection of f, an external signal . In the case of Figure 2 anomalous conditions are represented by the Δ block containing

some additional dynamics indicative of a type of failure or degradation. The ability to model anomalous conditions in these two ways proves indispensable in the application of the system-theoretic framework mentioned above.

1.1 Current Approaches to SSME Modeling

At this writing rocket engine dynamic modeling is anything but exact. This is readily apparent to anyone who has tried to read through the dearth of literature on the subject. Existing SSME models such as the RL00001, the RTM, the DTM, and the ROCETS package have been verified to some degree against hot fire test data. However, the approach taken in developing the dynamic equations in each case can be described as largely *ad hoc* and heavily reliant on empirical data. Such an approach necessitates the introduction of corrective parameters tuned to some standard mode of operation. Moreover, no method to date has proved useful in the development of models that can describe anomalous conditions, and this is critical in the development of model-based condition monitoring methods. The various chemical and thermal processes involved in a rocket engine are so complex that it is impossible to develop a model solely from first principles. Many researchers, therefore, resort to modeling based largely on empirical data. Models such as the RL00001, the RTM, the DTM, and ROCETS package were developed in this fashion. However, there are several shortcomings associated with this approach:

1. These models are often tuned to the data available and so they can become inaccurate when the modeled engine is slightly altered.

2. Often these models contain "correction" factors in the form of various coefficients necessary to get the model to match the observed data. For example, the various "B" coefficients employed in the RL00001, RTM, and DTM simulations. As a result, nobody but the one who developed the model understands the origin and or physical significance of these factors, and thus no one else can verify or build upon the model without some kind of support from the developer. In addition, there is no information inherent in the models that indicates why certain dynamics are kept while others are approximated by memoryless input/output relationships, a process known as residualization.

3. Although models such as the RTM and MARSYAS purport to be modular in design, the module interconnections are so complex that it becomes difficult to isolate certain components to study them separately or to compare them to other models.

4. Models are so complex that they become too cumbersome to use for control design purposes. Because of the *ad hoc* modeling method it is unclear how to reduce the modeling order without sacrificing fidelity to the actual engine.

5. Finally, these models are not easily used to study anomalous conditions, because it is difficult to know how to modify an empirical model to accurately account for modeling an actual anomaly.

For example, if one tries to compare Nguyen's SSME model [22], piece by piece, with Tiller's SSME model [30] few similarities will be found. This is due in large part to the inclusion of the so-called "corrective" parameters discussed above. A closer look at the dynamic "B" factors of the RTM reveals that for some of the flow equations the "B" coefficients governing dynamics differ by a factor of 100. One would hope that some of the dynamic equations could be residualized. However, some of the dynamic continuity equations are in terms of pressure while others in terms

of density. Comparing the magnitude of the dynamic "B" factors of these equations is meaningless as they are in terms of different units. The RTM HPFP is a good example of Item 3. The dynamic flow equation associated with the pump is composed of pressures and flows from various other components, some of which are dynamic. This makes it difficult to discern the actual boundaries of the pump model.

So, while each of these models may accurately replicate available nominal hot fire test data, the physical interpretations of the various internal variables is somewhat in question. Furthermore, these models are ill equipped to model anomalous conditions. Models with such limitations do not lend themselves easily for integrated health monitoring and control systems.

1.2 Control and Condition Monitoring Based Approach

A rigorous modeling method to describe quasi one-dimensional gaseous fluid flow through an arbitrary control volume has been previously developed [7] based on the conservation laws and thermodynamic laws and properties. The methodology cited above can be briefly described as follows: The mass, momentum and energy conservation laws and thermodynamic properties were cast in terms of common flow variables such as the pressure, temperature and velocity of the fluid in the control volume. The resulting partial differential equations (PDE's) were reformulated in terms of Mach number and made computationally tractable by shedding their dependence on a particular system of units via a process called nondimensionalization and by a conversion to ordinary differential equations via a novel spatial discretization. The how and why of the nondimensionalization and discretization procedures adopted for our purposes is discussed in detail in Sections 7 and 8.

This method has been successfully applied in modeling the high frequency transient dynamics associated with turbomachinery such as air-breathing turbojet engines [6, 5]. This modeling scheme combines in a rigorous fashion modeling techniques based upon first principles and modeling techniques based upon empirical data when first principles are too difficult to apply. The advantage of this is that first principle models are easier to manipulate and extend to model a wide variety of states/conditions and anomalous behaviors for the system being modeled. When it is too difficult to apply first principles, for example the pump maps associated with turbopumps, we can use steady state experimentation to determine appropriate forcing terms which can be incorporated into the model yet still maintain the structure and uniformity. Models generated using this approach possess the following advantages over the existing models discussed in Section 1.1:

1. Changes in the operation of the physical system can be accommodated by modifying only the steady state input/output maps leaving the rest of the model unaltered.

2. Because of the rigorous method, the models contain no vague "correction" factors and are quite structured. Each part of the models is either derived from first principles or obtained through steady state experimentation. Someone wishing to verify or build upon these models should be able to do so without support from the developer.

3. System models are made up of distinct components with well-defined boundaries and interconnections.

4. The potential to reduce the model order is inherent in the models making them suitable for control design purposes.

5. Most importantly for integrated control and condition monitoring, these models are equipped to handle anomalous conditions in a rigorous manner.

In this work, the above methods are extended to handle liquid fluid flows thereby yielding modeling methods which can be applied to liquid rocket engines systems. In addition, it is discussed how these methods can be applied to develop models which describe the nominal operation of rocket systems as well as models describing various anomalous or degraded rocket engine systems. As such this work provides rigorous methods for control and condition monitoring oriented rocket engine modeling.

1.3 Research Assistants

Please note that the work presented herein is a result of a collaborative effort between Primary Investigator Dr. Helmicki, and Graduate Research Assistants Sayeed Jaweed and Ksenia Kolcio. Both students work in the Applied Systems Research Lab headed by Dr. Helmicki. Sayeed Jaweed and Ksenia Kolcio are pursuing Ph.D. and Master's Theses, respectively. Some of the results of this document will contribute directly to their theses. This research project has led to the following four conference papers:

1. A. Helmicki, S. Jaweed, and K. Kolcio; An Integrated Approach to Rocket Condition Monitoring and Control.

   Appeared in the Fourth Annual Space System Health Management Technology Conference, 1992

2. A. Helmicki, S. Jaweed, and K. Kolcio; Propulsion System Modelling for condition Monitoring and Control: A Status Report.

   Appearing in the SAE 1994 Aerospace Atlantic Conference and Exposition

3. A. Helmicki, S. Jaweed, and K. Kolcio; Liquid Rocket Engine Modeling for Control and Condition Monitoring: Part I, Theoretical Foundations.

   Appearing in the 1994 JPC

4. A. Helmicki, S. Jaweed, and K. Kolcio; Liquid Rocket Engine Modeling for Control and Condition Monitoring: Part II, Application to the Space Shuttle Main Engine.

   Appearing in the 1994 JPC

2 Summary

A rigorous propulsion system modelling method suitable for control and condition monitoring purposes is developed. Previously developed control oriented methods yielding nominal models for gaseous medium propulsion systems are extended to include both nominal and *anomalous* models for *liquid* mediums in the following two ways. First, thermodynamic and fluid dynamic properties for liquids such as liquid hydrogen are incorporated into the governing equations. Second, anomalous conditions are captured in ways compatible with existing system theoretic design tools so that anomalous models can be constructed. Control and condition monitoring based methods are seen as an improvement over some existing modelling methods because such methods typically do not rigorously lead to low order models nor do they provide a means for capturing anomalous conditions. Applications to the nominal SSME HPFP and degraded HPFP serve to illustrate the approach.

3 Overview

An equation needed to relate thermodynamic properties for a liquid is developed in Section 5 and incorporated into the mass, momentum and energy conservation equations in Section 6 yielding a set of partial differential equations able to describe the flow of LH_2 and LOX through an arbitrary control volume.

Section 7 reformulates these equations into a more compact form where the states are given by the standard flow variables: Mach number, pressure and temperature and renders them independent of the choice of basic units through the use of a nondimensionalization scheme. An added feature of this nondimensionalization scheme is that it provides some insight into the dynamic behavior of the differential equations.

Once the general dimensionless flow equations are developed, the control and condition monitoring based techniques are discussed in Sections 8-9 resulting in a general model applicable to liquid fluid flow systems. The equations are first discretized in Section 8 following the successful approach used in [7] to arrive at a system of ordinary differential equations. Then in Section 9 decisions are made regarding the choice of inputs and outputs to the model.

Section 11 applies this method developed in the previous sections to discuss the development of a low order dynamic nominal model of the SSME HPFP.

Section 12 shows how the nominal HPFP model can be augmented with the signal and uncertainty representations introduced in Section 1 to include particular anomalous conditions.

4 Nomenclature

Here the various symbols and notation appearing throughout this work are listed for easy reference.

A	area	T	temperature
c	orifice coefficient	t	time
DW	mass flow	c_v	constant volume specfic heat
e	internal energy	u	fluid velocity
f	force	x	position
S	shaft speed	α	cubical expansion coefficient
L	length	β	isothermal bulk modulus
M	Mach number	ϵ	dynamic dimensionless parameter
P	pressure	γ	dimensionless parameter
Q	rate of heat transfer	χ	dimensionless parameter
R	gas constant	ρ	density
LOX	liquid oxygen	LH_2	liquid hydrogen

The various subscripts and superscripts used will be defined as the need arises. It is important to note that throughout this work a distinction is made between variables having units (dimensional) and those void of units (nondimensional). From here on, the $\bar{}$ symbol over the dimensional variables differentiates them from their nondimensional counterparts.

5 Equation of State for LH_2 and LOX

Before the control and condition monitoring approach can be applied to liquid rocket engines, the equations developed in [7] for gaseous flows must be augmented to accommodate liquid flows.

The development of the modeling techniques referenced in [7, 6, 5] relies on the use of the ideal gas law. Consequently the models thus developed are not applicable to all components of a liquid rocket engine such as the SSME because LH_2 and LOX do not obey the ideal gas law. This section develops a new thermodynamic state equation for a liquid such as LH_2 or LOX that agrees with empirical data found in [20].

For a liquid the ideal gas law

$$\tilde{P} = \tilde{\rho}\tilde{R}\tilde{T} \tag{1}$$

no longer applies. Unfortunately no equation of state (EOS) relating density to pressure and volume of an arbitrary liquid exists [21]. All such equations come about using empirical methods [17, 27, 12, 2, 28], and each equation is tailored to describe the density of a specific set of fluids. As well, many of the equations from the literature are useful only in limited ranges of the pressure, density, and temperature surface of a particular fluid. For example, a two-parameter equation of state developed in [12] was verified for liquid hydrocarbons, but not for LH_2; and the Van der Waals equation reviewed in [27] works for gaseous hydrogen but is not recommended for the liquid region.

The SSME HPFP experiences large pressure and temperature variations from inlet to outlet. At 109% Rated Power Level (RPL), the inlet pressure and temperature are about 350 psi (pounds per square inch) and 26 K (degrees Kelvin), while the output pressure and temperature of the HPFP are about 6870 psi and 56 K, respectively. The HPFP inlet to outlet pressure and temperature range given above will be referred to as simply the operating range.

With such large pressure and temperature variations, one would not expect any one equation to cover the entire range. Indeed, as evidenced by Figure 3, the equation given in [20] for LH_2 does not fit the empirical data in the operating range of the SSME HPFP.

Following the modelling scheme of this work, first principles facilitate the derivation of the EOS used here. The EOS takes the form $\tilde{\rho} = f(\tilde{P}, \tilde{T})$. The total differential of density can be written [11] as

$$d\tilde{\rho} = \left(\frac{\partial\tilde{\rho}}{\partial\tilde{T}}\right)_P d\tilde{T} + \left(\frac{\partial\tilde{\rho}}{\partial\tilde{P}}\right)_T d\tilde{P} \,. \tag{2}$$

This equation can be simplified by noting that the isothermal bulk modulus β is defined as [11]

$$\beta := \tilde{\rho}\left(\frac{\partial\tilde{P}}{\partial\tilde{\rho}}\right)_T \,,$$

and that the cubical expansion coefficient or coefficient of volume expansion α is defined as [11]

$$\alpha := -\frac{1}{\tilde{\rho}}\left(\frac{\partial\tilde{\rho}}{\partial\tilde{T}}\right)_P \,.$$

Substituting these definitions, Equation 2 then becomes

$$\frac{d\tilde{\rho}}{\tilde{\rho}} = \frac{1}{\beta}d\tilde{P} - \alpha d\tilde{T} \,.$$

Integration from $(\bar{\rho}, \bar{P}, \bar{T})$ to $(\tilde{\rho}, \tilde{P}, \tilde{T})$ yields

$$\ln\left(\frac{\tilde{\rho}}{\bar{\rho}}\right) = \frac{1}{\beta}(\tilde{P} - \bar{P}) - \alpha(\tilde{T} - \bar{T})$$

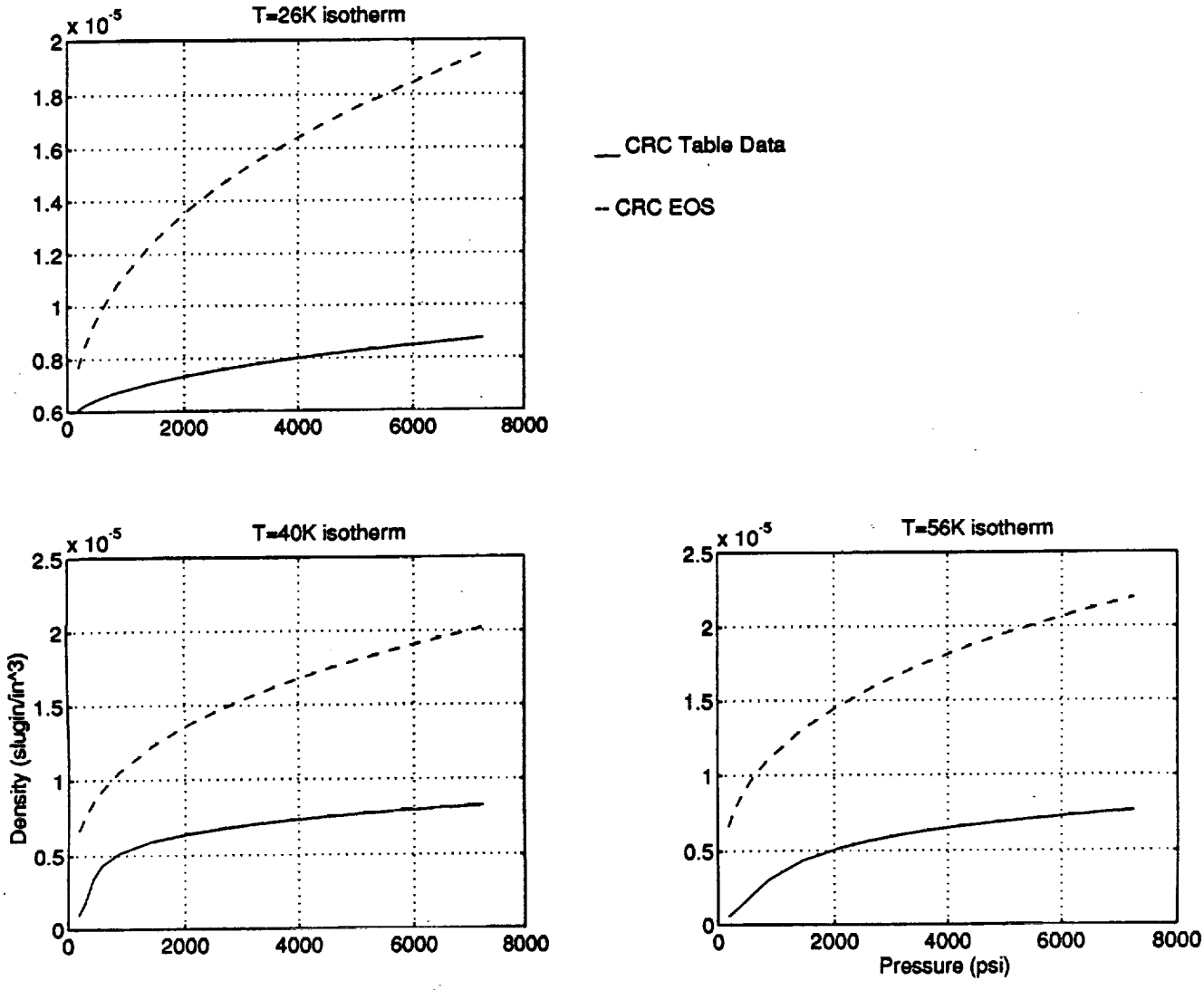

Figure 3: Comparison of CRC EOS and empirical data.

where $\bar{\rho}$, $\bar{P}$, $\bar{T}$ are reference values. Isolating density in this expression yields

$$\tilde{\rho} = \kappa e^{(\frac{1}{\beta}\tilde{P} - \alpha\tilde{T})}, \tag{3}$$

where the reference values have been collected into the constant term κ.

Figure 4 gives plots of this EOS against the empirical data found in [20]. Comparing these plots

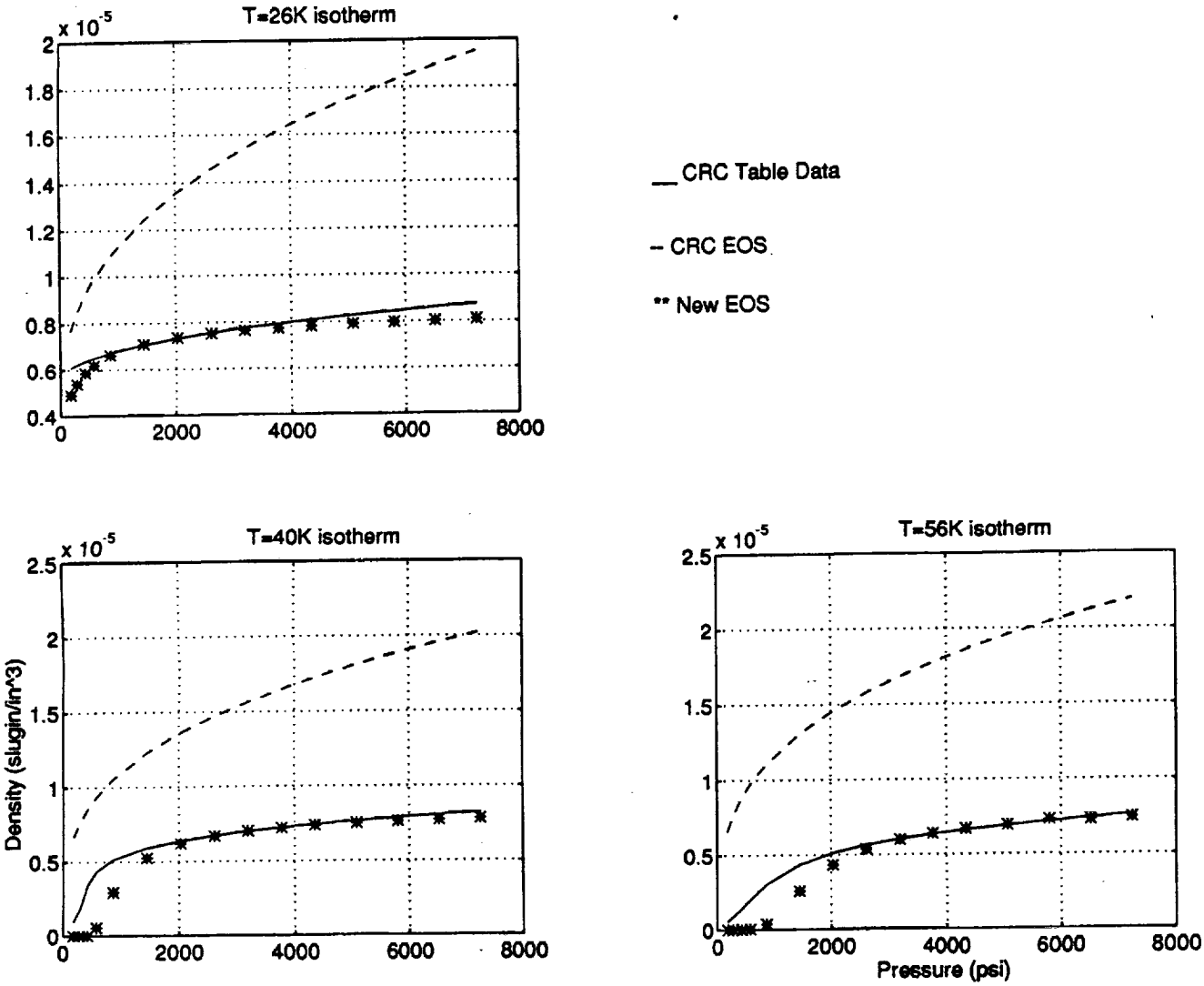

Figure 4: Comparison of CRC EOS and new EOS both against empirical data.

with those of Figure 3 it can be seen that this EOS provides a better fit than those given in [20].

Now a few words about the choice of reference values and the α and β parameters. The reference parameters, $\bar{\rho}$, $\bar{P}$ and $\bar{T}$, were chosen from the approximate mid point of the operating range. The α and β parameters actually vary with pressure and temperature. However, in order to simplify the integration step above, the parameters were first assumed constant with respect to pressure and temperature. The constant α and β were obtained as described next. From each operating range pressure and temperature entry in the empirical tables in [20], a corresponding α entry was

extracted. A vector of these α values was then averaged to yield a mean α. Similarly, a mean β was calculated. These mean α and β values were then used in the derivation of Equation 3. Similar results apply in the case where LOX is considered. Next, the conservation equations are introduced and the new EOS is combined with them.

6 Dynamic Fluid Flow Through a Control Volume

The well-known differential forms of the dimensional continuity, momentum and energy equations for quasi one-dimensional, fluid flow through a variable area control volume are given respectively, as [31, 7, 4]

$$\frac{\partial}{\partial \tilde{t}}(\tilde{\rho}\tilde{A}) = -\frac{\partial}{\partial \tilde{x}}(\tilde{\rho}\tilde{u}\tilde{A}) \,, \tag{4}$$

$$\frac{\partial}{\partial \tilde{t}}(\tilde{\rho}\tilde{u}\tilde{A}) + \frac{\partial}{\partial \tilde{x}}(\tilde{\rho}\tilde{u}^2 A) = -\tilde{A}\frac{\partial \tilde{P}}{\partial \tilde{x}} + \tilde{\rho}\tilde{A}\tilde{f}_s + \tilde{\rho}\tilde{A}\tilde{f}_w \,, \tag{5}$$

$$\frac{\partial}{\partial \tilde{t}}[\tilde{\rho}\tilde{A}(\tilde{e} + \frac{\tilde{u}^2}{2})] + \frac{\partial}{\partial \tilde{x}}[(\tilde{\rho}\tilde{u}\tilde{A}(\tilde{e} + \frac{\tilde{u}^2}{2})] = -\frac{\partial}{\partial \tilde{x}}(\tilde{u}\tilde{P}\tilde{A}) + \tilde{\rho}\tilde{A}\tilde{u}\tilde{f}_s + \tilde{A}\tilde{Q} \,. \tag{6}$$

The variables used in these equations are defined in Table 1.[1] These equations hold at each point in an arbitrary control volume.

Equation 4 maintains that the time rate of change of mass in a control volume (CV),

$$\frac{\partial}{\partial \tilde{t}}(\tilde{\rho}\tilde{A}) \,,$$

must equal the mass flow through the CV,

$$-\frac{\partial}{\partial \tilde{x}}(\tilde{\rho}\tilde{u}\tilde{A}) \,.$$

Equation 5 restates Newton's second law that the total rate of change of momentum in the CV,

$$\frac{\partial}{\partial \tilde{t}}(\tilde{\rho}\tilde{u}\tilde{A}) + \frac{\partial}{\partial \tilde{x}}(\tilde{\rho}\tilde{u}^2) \,,$$

must equal the sum of the force due to pressure on the CV,

$$-\tilde{A}\frac{\partial \tilde{P}}{\partial \tilde{x}} \,,$$

the force due to wall friction,

$$\tilde{\rho}\tilde{A}\tilde{f}_w$$

and the force due to some shaft moving through the fluid,

$$\tilde{\rho}\tilde{A}\tilde{f}_s \,.$$

Finally, Equation 6 states that the time rate of change of energy in the CV,

$$\frac{\partial}{\partial \tilde{t}}[\tilde{\rho}\tilde{A}(\tilde{e} + \frac{\tilde{u}^2}{2})] \,,$$

plus the net flow of energy through the CV,

$$\frac{\partial}{\partial \tilde{x}}[(\tilde{\rho}\tilde{u}\tilde{A}(\tilde{e} + \frac{\tilde{u}^2}{2})] \,,$$

must equal the sum of the rate of the shaft work and pressure work done inside the CV,

$$-\frac{\partial}{\partial \tilde{x}}(\tilde{u}\tilde{P}\tilde{A}) + \tilde{\rho}\tilde{A}\tilde{u}\tilde{f}_s \,,$$

Variable	*Description*
$\tilde{\rho}$	density $(lbf - sec^2/in^4)$
$\tilde{P}$	pressure (lbf/in^2)
$\tilde{T}$	temperature $(Rankine, R)$
$\tilde{u}$	velocity (in/sec)
$\tilde{x}$	position (in)
$\tilde{t}$	time (sec)
$\tilde{A}$	cross-sectional area (in^2)
$\tilde{e}$	internal energy (in^2/sec^2)
$\tilde{Q}$	heat transfer rate $(lbf/sec - in^2)$
$\tilde{f}_s$	shaft-on-fluid forces (in/sec^2)
$\tilde{f}_w$	wall-on-fluid friction (in/sec^2)

Table 1: Dimensional variables.

plus the rate of heat added to the CV, $\tilde{A}\tilde{Q}$. Note that the wall friction does not appear in the energy equation because the friction acts at a point in the flow where the velocity is zero and hence no work is done.

Along with Equations 4, 5, 6, and 3, the well known thermodynamic equation relating the internal energy and temperature

$$\tilde{e} = c_v \tilde{T}$$

complete the set of equations governing unsteady, compressible, viscous, quasi one-dimensional flow of a liquid such as LH_2 or LOX. These equations, because of the partial derivatives with respect to position and variables such as internal energy and density, do not lend themselves easily in solving fluid dynamic problems. The goal is to first reformulate these equations in terms of the usual flow variables, pressure, temperature and velocity and then to approximate somehow the partial derivatives with respect to position. After eliminating the internal energy and simplifying, the following equations result:

$$\begin{aligned}
\frac{\partial \tilde{\rho}}{\partial \tilde{t}} &= -\tilde{\rho}\frac{\partial \tilde{u}}{\partial \tilde{x}} - \tilde{u}\frac{\partial \tilde{\rho}}{\partial \tilde{x}} - \frac{\tilde{\rho}\tilde{u}}{\tilde{A}}\frac{\partial \tilde{A}}{\partial \tilde{x}} - \frac{\tilde{\rho}}{\tilde{A}}\frac{\partial \tilde{A}}{\partial \tilde{t}}\,, \\
\frac{\partial \tilde{u}}{\partial \tilde{t}} &= -\tilde{u}\frac{\partial \tilde{u}}{\partial \tilde{x}} - \frac{1}{\tilde{\rho}}\frac{\partial \tilde{P}}{\partial \tilde{x}} + \tilde{f}_s + \tilde{f}_w\,, \\
\frac{\partial \tilde{T}}{\partial \tilde{t}} &= -\tilde{u}\frac{\partial \tilde{T}}{\partial \tilde{x}} - \frac{\tilde{P}}{\tilde{\rho}c_v}\frac{\partial \tilde{u}}{\partial \tilde{x}} - \frac{\tilde{P}\tilde{u}}{\tilde{A}\tilde{\rho}c_v}\frac{\partial \tilde{A}}{\partial \tilde{x}} + \frac{\tilde{Q}}{\tilde{\rho}c_v}\,.
\end{aligned}$$

At this point the EOS could be substituted in for the density and the result solved for the pressure. However, due to the complexity of the EOS, first transforming the dimensional variables to nondimensional ones proves simpler. Section 7 explains this nondimensionalization process.

[1]Note that here body forces such as electromagnetic and gravitational forces have been ignored and/or assumed negligible.

7 Nondimensionalization

Historically, nondimensionalization has been employed in scale models [29] and in the reduction of parameters needed for solutions [18]. In fluid dynamics, the nondimensionalization process yields nondimensional parameters such as the Reynolds number, Re. The size of Re determines whether laminar or turbulent flow is to be assumed. Because of the nondimensional nature of Re, not only does its numerical value stay the same in the face of a change of units but different fluid dynamic systems in different units can be compared using their respective Reynolds numbers. Most recently, the advantages of nondimensionalization have been applied to dynamic system modelling [7, 6, 5, 8] to gain more insight into dynamic behavior. A nondimensionalizing scheme eliminates the need to keep track of units and transforms the equations to a more elegant form. The dimensionless variables employed herein are defined in Table 2.

Variable/Parameter	*Description*
$\rho = \ln\left(\frac{\tilde{\rho}}{\kappa}\right)$	dimensionless density
$P = \frac{\tilde{P}}{\beta}$	dimensionless pressure
$T = \alpha\tilde{T}$	dimensionless temperature
$M = \tilde{u}/\sqrt{\frac{\beta}{\tilde{\rho}}}$	Mach number
$x = \tilde{x}/\bar{L}$	dimensionless position
$t = \tilde{t}/\bar{t}$	dimensionless time
$A = \tilde{A}/\bar{A}$	dimensionless area
$\epsilon = \frac{\bar{t}}{\bar{L}}\sqrt{\frac{\beta}{\kappa}}\, e^{\frac{T-P}{2}}$	dimensionless dynamic factor
$f_s = \frac{\alpha\bar{L}}{c_v}\tilde{f}_s$	dimensionless shaft force
$f_w = \frac{\alpha\bar{L}}{c_v}\tilde{f}_w$	dimensionless friction force
$Q = \frac{\alpha\bar{L}}{c_v\beta}\tilde{Q}$	dimensionless heat transfer
$\gamma_1 = \frac{\beta}{\kappa e^{T-P}}$	dimensionless parameter
$\gamma_2 = \frac{\kappa c_v}{\beta\alpha}$	dimensionless parameter

Table 2: Nondimensional variables and Parameters

The process proceeds as follows: First, the EOS, Equation 3, is nondimensionalized and used to eliminate density from the expressions. Second, the remaining variable substitutions are made and algebraic manipulations are used to simplify the resulting equations. Because of the complex nature of these computations, this nondimensionalization process was accomplished with the help of the symbolic math software package, Mathematica [34]. Below is the result of this procedure presented in matrix form:

$$\frac{1}{\epsilon}\frac{\partial}{\partial t}\begin{bmatrix} M \\ P \\ T \end{bmatrix} = \Gamma(M,\chi)\frac{\partial}{\partial x}\begin{bmatrix} M \\ P \\ T \end{bmatrix} + \Lambda(\gamma_1,\gamma_2)\begin{bmatrix} f_s \\ f_w \\ Q \end{bmatrix} + \Theta(M,\chi,A)\frac{\partial A}{\partial x} + \frac{1}{\epsilon}\Omega(M,\chi,A)\frac{\partial A}{\partial t}, \tag{7}$$

where

$$\epsilon = \frac{\bar{t}}{\bar{L}}\sqrt{\frac{\beta}{\kappa}}\, e^{\frac{T-P}{2}},$$

$$\Gamma(M,\chi) = \begin{bmatrix} -\frac{3}{2}M & \frac{M^2}{4}-1 & -\frac{M^2}{4} \\ -(\chi+1) & \frac{M}{2}(\chi-1) & -\frac{M}{2}(\chi+1) \\ -\chi & \frac{M}{2}\chi & -M(\frac{\chi}{2}+1) \end{bmatrix},$$

$$\Lambda(\gamma_1,\gamma_2) = \begin{bmatrix} \gamma_2 & \gamma_2 & 0 \\ 0 & -M & \sqrt{\gamma_1} \\ 0 & -M & \sqrt{\gamma_1} \end{bmatrix},$$

$$\Theta(M,\chi,A) = \begin{bmatrix} -\frac{M^2}{2A} \\ -\frac{M}{A}(\chi+1) \\ -\frac{M}{A}\chi \end{bmatrix}, \quad \Omega(M,\chi,A) = \begin{bmatrix} -\frac{M}{2A} \\ -\frac{1}{A} \\ 0 \end{bmatrix},$$

$$\gamma_1 = \frac{\beta}{\kappa e^{P-T}}, \quad \gamma_2 = \frac{\kappa c_v}{\beta\alpha}, \quad \chi = \frac{\alpha P\sqrt{\gamma_1}}{c_v}.$$

Matrix Equation 7 describes the dynamics of liquid fluid flow in terms of three nondimensional equations relating three nondimensional fluid flow variables. The study of these equations leads to several insights in behavior of liquid fluid flows and their dynamics. Consider the term ϵ which appears as a coefficient of each of the left hand side matrix terms of Equation 7. Note that ϵ has physical meaning in that the term $\sqrt{\beta/\kappa}$ is a reference speed of sound determined by the properties β and κ of the liquid. In dimensional variables $\epsilon = \frac{\bar{t}}{\bar{L}}\sqrt{\frac{\bar{\beta}}{\bar{\rho}}}$. This is similar to the dimensionless parameter employed in fluid transients called the Strouhal number which is the ratio of length to mean velocity and fluid oscillation period [19].

The ϵ parameter controls the speed of the dynamic response of these equations. Since ϵ appears in front of all three equations it serves as a "system" parameter in that depending on its size, all the dynamics are either kept or residualized. The fact that ϵ appears in all three equations is a direct consequence of the nondimensionalization procedure. For ϵ relatively large the dynamics equilibrate quickly, reaching steady state essentially instantaneously. In this case, the dynamics are residualized meaning that they are reduced to memoryless input/output relationships. For ϵ relatively small the dynamics are slower, taking a significant amount of time to reach steady state. For this case, the dynamics are retained. Although the residualized equations have the same form as steady state relationships they have quite a different meaning. Residualized equations are algebraic and apply at each point in time while steady state relationships apply only after transient effects have died away. So for residualized equations the algebraic input/output relationships can be applied at some initial time, $t = t_0$ while for equations where dynamics are retained, the steady state relationships can be applied only after some appropriate $t > t_0$. Thus, depending on the size of ϵ the possibility exists for the dynamic order of a component model to be reduced. Two other dimensionless parameters of interest are γ_1, γ_2 and χ. Their relative sizes may cause certain terms such as the forcing terms to drop out. Such simplifications can greatly reduce the overall model complexity for multi-component models.

8 Discretization

Spatial discretization of the nondimensionalized PDE's developed above is necessary in order to be able to easily code the equations for computer simulation purposes. Spatial discretization serves to change the PDE to an ordinary differential equation via some approximation of the spatial partial derivative. Here, the same discretization method introduced in [7] is employed.

First the entire system is compartmentalized into components employing natural boundaries. For example, in the SSME various components would include the HPFP, the HPOP, the combustion chamber and the injectors, to name a few. Next, the spatial domain of each component is split into n elements. For some components a single element will suffice, while for others more than one may be necessary. The entrance to the first element is demarcated by x_0 while the exit of the last element is x_n. It is then assumed that the variables with spatial derivatives vary linearly across the element. The linear distributions take the following form

$$\begin{aligned} M(x,t) &= M_{k-1}(t) + [M_k(t) - M_{k-1}(t)](x - x_{k-1}) , \\ P(x,t) &= P_{k-1}(t) + [P_k(t) - P_{k-1}(t)](x - x_{k-1}) , \\ T(x,t) &= T_{k-1}(t) + [T_k(t) - T_{k-1}(t)](x - x_{k-1}) , \\ A(x,t) &= A_{k-1}(t) + [A_k(t) - A_{k-1}(t)](x - x_{k-1}) , \end{aligned}$$

where $M_k(t) := M(x_k, t)$ and x_{k-1} is at the entrance to the kth element while x_k is at the exit and $k \in [1, \ldots, n]$. The same definition applies for $P_k(t)$, $T_k(t)$ and $A_k(t)$. Note that t and x are the only variables in the above equations. The positions x_{k-1} and x_k are fixed at the entrance and exit, respectively, of the kth element. The difference of the variables across the element approximates the spatial derivative of the variable. After taking the derivative of the above with respect to x, the spatial derivatives can then be approximated by

$$\begin{aligned} \frac{\partial}{\partial x} M &\approx M_k(t) - M_{k-1}(t) , \\ \frac{\partial}{\partial x} P &\approx P_k(t) - P_{k-1}(t) , \\ \frac{\partial}{\partial x} T &\approx T_k(t) - T_{k-1}(t) , \\ \frac{\partial}{\partial x} A &\approx A_k(t) - A_{k-1}(t) . \end{aligned}$$

Once the spatial derivatives have been approximated, the resulting equations are valid at any point in the spatial domain of the element. This is a consequence of the linear distribution assumption as the spatial derivative is a constant. Even if the spatial distribution proves not to be linear across an element for a certain value of n then n can be sufficiently increased until a linear approximation is valid. Substituting these discretized spatial derivatives into Equation 7 yields

$$\begin{aligned} \frac{1}{\epsilon}\frac{d}{dt}\begin{bmatrix} M \\ P \\ T \end{bmatrix} &= \Gamma(M,\chi)\begin{bmatrix} M_k - M_{k-1} \\ P_k - P_{k-1} \\ T_k - T_{k-1} \end{bmatrix} + \Lambda(\gamma_1,\gamma_2)\begin{bmatrix} f_s \\ f_w \\ Q \end{bmatrix} \\ &+ \Theta(M,\chi,A)(A_k - A_{k-1}) + \frac{1}{\epsilon}\Omega(M,\chi,A)\frac{dA}{dt} . \end{aligned}$$

These equations apply to each of the n elements of a component or subsystem. For each element three dynamic equations result. For a component or subsystem, then, that makes $3n$

9 State Assignment

The discretization process divided the system into components along natural boundaries. Some configuration of the inlets and outlets of the physical components are used as the inputs and outputs of the model. Care should be taken so that the choice of inputs and outputs make sense physically. This has potentially important ramifications when the problems of sensor and actuator placement are considered.

Typically, outlet Mach numbers are either known to be a certain value or at least desired to be a certain value. In other words, $M_k(t)$ is an input. For this reason the temporal derivative of Mach number, $\partial M/\partial t$, is evaluated at the entrance of the element, forcing $M_{k-1}(t)$ to be a state. Similarly, inlet pressures and temperatures are usually known. Therefore $\partial P/\partial t$ and $\partial T/\partial t$ are evaluated at the exit of each element, forcing $P_k(t)$ and $T_k(t)$ to be states. The rest of the terms in Equations 8 are evaluated at $x = x_k$ for M and at $x = x_{k-1}$ for P and T. Evaluating some temporal derivatives at $x = x_k$ and other variables at $x = x_{k-1}$ is acceptable because in the limit as the spatial mesh becomes finer and finer, x_{k-1} approaches x_k.

Using the state assignment scheme just discussed the discretized equations for the kth element of the spatial domain become

$$\frac{1}{\epsilon}\frac{d}{dt}\begin{bmatrix} M_{k-1} \\ P_k \\ T_k \end{bmatrix} = \Gamma(M_k, \chi_{k-1})\begin{bmatrix} M_k - M_{k-1} \\ P_k - P_{k-1} \\ T_k - T_{k-1} \end{bmatrix} + \Lambda(\gamma_1, \gamma_2)\begin{bmatrix} f_s \\ f_w \\ Q \end{bmatrix} + \Theta(M_k, \chi_{k-1}, A_{k-1})(A_k - A_{k-1}) + \frac{1}{\epsilon}\Omega(M_k, \chi_{k-1}, A_{k-1})\frac{dA}{dt}, \quad (8)$$

and

$$\epsilon = \frac{\bar{t}}{\bar{L}}\sqrt{\frac{\beta}{\kappa}}\, e^{\frac{T_{k-1}-P_{k-1}}{2}}.$$

Equations 8 comprise a general set of equations able to model a generic fluid dynamic system or component. In the next section we discuss the forcing terms.

PRECEDING PAGE BLANK NOT FILMED

PAGE 18 INTENTIONALLY BLANK

10 Forcing Terms

In general, the forcing terms are functions of all the flow variables, their spatial and temporal partial derivatives, the various parameters and inputs and the system geometry. If it is assumed that the dependence is only on the flow variables, parameters, external inputs and geometry, then

$$\begin{aligned} f_s &= f_s(M, P, T, A, \bar{L}, c_v, \alpha, \beta, \kappa, external\ inputs)\ , \\ f_w &= f_w(M, P, T, A, \bar{L}, c_v, \alpha, \beta, \kappa, external\ inputs)\ , \\ Q &= Q(M, P, T, A, \bar{L}, c_v, \alpha, \beta, \kappa, external\ inputs)\ . \end{aligned}$$

External inputs could include the ambient pressure and the pump shaft speed of the HPFP, for example. Assuming no dependence on $\frac{\partial M}{\partial x}$ eliminates fluid on fluid viscous forces but retains shaft-on-fluid and wall-on-fluid frictional forces. Now, the particular discretization method chosen above demands that all variables in the Γ, Λ, Θ and Ω matrices and variables in the forcing functions be evaluated at the inputs. The forcing functions then have the form

$$\begin{aligned} f_s &= f_s(M_k, P_{k-1}, T_{k-1}, A_{k-1}, A_k, \bar{L}, c_v, \alpha, \beta, \kappa, external\ inputs)\ , \\ f_w &= f_s(M_k, P_{k-1}, T_{k-1}, A_{k-1}, A_k, \bar{L}, c_v, \alpha, \beta, \kappa, external\ inputs)\ , \\ Q &= Q(M_k, P_{k-1}, T_{k-1}, A_{k-1}, A_k, \bar{L}, c_v, \alpha, \beta, \kappa, external\ inputs)\ . \end{aligned}$$

Forcing terms are defined in one of two ways: either known forms are assumed, for example Fanno, Raleigh or isentropic area change, or unknown forcing terms are determined through steady state input/output experiments. If the form of the functions is unknown, we turn to steady state experiments to obtain input-output maps. It is common practice in turbomachinery applications to make use of nondimensional pump and torque maps to characterize the pressure rise across pumps and shaft torque as a function of flow variables and shaft speed absorbed into a dimensionless variable [32, 10]. The pressure rise across the SSME turbopumps is found in terms of such nondimensional pump maps.

The dynamic equations must be manipulated so that the maps resulting from input-output experiments can be folded back into the dynamic equations. To this end, let the functions f_1, f_2 and f_3 be defined by

$$\begin{bmatrix} f_1 \\ f_2 \\ f_3 \end{bmatrix} := -\Gamma^{-1}\Lambda \begin{bmatrix} f_s \\ f_w \\ Q \end{bmatrix} - \Gamma^{-1}\Theta(A_k - A_{k-1})\ .$$

The new functions f_1, f_2, f_3 depend on the same variables as f_s, f_w and Q with the addition of $(A_k - A_{k-1})$ through the second term in the above equation. Substituting these functions back into Equation 8 gives

$$\begin{aligned} \frac{1}{\epsilon}\frac{d}{dt}\begin{bmatrix} M_{k-1} \\ P_k \\ T_k \end{bmatrix} = \Gamma(M_k, \chi_{k-1})\left\{\begin{bmatrix} M_k - M_{k-1} \\ P_k - P_{k-1} \\ T_k - T_{k-1} \end{bmatrix} - \begin{bmatrix} f_1 \\ f_2 \\ f_3 \end{bmatrix}\right\} \\ + \frac{1}{\epsilon}\Omega(M_k, \chi_{k-1}, A_{k-1})\frac{d}{dt}A_k\ . \end{aligned} \tag{9}$$

In steady state, the time derivatives in Equation 9 vanish and the following should be satisfied

$$\begin{bmatrix} M_k - M_{k-1} \\ P_k - P_{k-1} \\ T_k - T_{k-1} \end{bmatrix} = \begin{bmatrix} f_1 \\ f_2 \\ f_3 \end{bmatrix}\ . \tag{10}$$

These functions can be obtained via steady state experiments provided that the full domain of input variables can be traversed in steady state.

Restricting the functions to depend on inputs only rather than states allows explicit determination of these forms. If the functions were allowed to depend on states as well as inputs, then they could not be determined from steady state experiments. For example, suppose that $n = 1$ and the only forcing function happens to be $f_1(M_0, P_0, T_0)$ which depends on the state variable, M_0. In steady state

$$M_1 - M_0 = f1(M_0, P_0, T_0)$$

should be satisfied. However, if one were to attempt to run steady state input/output experiments one could not simultaneously traverse the domain of M_0 values as inputs to f_1 and record the corresponding M_0 output values.

The next task is to apply the set of equations derived above to a specific system using the control and condition monitoring based approach. This approach can be outlined as follows:

Step 1:

The physical system is conceptually divided into distinct interconnected components. For example, the HPFP is one component of the physical system the SSME. If necessary, each component is further subdivided into finite elements. The dimensionless flow equations are applied to each element of every component.

Step 2:

For each element, the discretization and state assignment scheme is utilized to obtain a nominal lumped parameter model.

Step 3:

For elements having nonzero forcing terms, relations describing these forcing terms are either determined from first principles or from steady state experiments.

Step 4:

Based on the relative size of the ϵ parameter resulting from the nondimensionalization, a decision is made to either residualize or retain the flow dynamics for each element.

Step 5:

The developed models for all system elements are aggregated to form the overall nominal system model.

Step 6:

Depending on the nature of the anomalies, anomalous conditions are introduced to the model as either additional dynamics or injected signals.

The dynamic dimensional flow equations for Step 1 have been developed in Sections 5- 7. Step 2 was discussed in Sections 8- 9. The next two sections deal with Steps 3-6. In these sections, the generic equations generated above are used to model the SSME HPFP in order to illustrate their application. Section 11 describes the nominal model and Section 12 describes models able to characterize certain anomalous conditions.

11 SSME HPFP Nominal Model

The SSME HPFP is a three staged centrifugal pump. The turbine generates the available torque to turn the pump shaft. Liquid hydrogen fuel enters the pump at the inlet volute, courses through the pump stages where the kinetic energy of the flow is converted to potential energy (pressure), and exits at the outlet volute. The purpose of the pump is to compress the fuel to a high enough pressure so that it may enter the combustion chamber.

For simplicity, it is assumed for now that the entire HPFP can be modeled as one element. Following the notation of Section 7, a one element component means that $k = 1$. The pump inlet pressure, P_0, and temperature, T_0, and the Mach number at the pump outlet, M_1, serve as the model inputs while the pump outlet pressure, P_1, and temperature, T_1, and Mach number at the inlet, M_0, become the states and outputs of the model. If it is determined that more than one element is necessary, each pump stage can be modeled as an element. The elements would then be concatenated to form the entire HPFP. Increasing the number of elements means that additional pump maps would be needed for each compressor stage in order to determine the forcing functions. From a practical standpoint, obtaining these maps is not a trivial task. Thus, the classic trade-off between theory and practice is incurred. The same procedure would be applied to the turbine only using the equations derived for a gaseous fluid. The HPFP and turbine models together would comprise the High Pressure Fuel Turbopump, HPFTP.

Some general assumptions are in order. As flow through the pump is assumed to be adiabatic, heat transfer is negligible so the Q term drops out. Fluid-on-fluid forces are negligible so the f_s term covers shaft forces exclusively. However, wall-on-fluid friction forces exist and appear in the f_w term. Since there are no valves within the HPFP, the time derivative of area drops out of the nominal model. To determine the f_s and f_w terms either some particular functional forms must be assumed or maps derived through an analysis of the SSME steady state operation which is well understood. In the SSME RTM and the SSME MARSYAS models the pressure rise generated by the pump comes from steady state pump maps [22, 30]. Here, instead of choosing a functional form for f_s we attempt to fold in the existing HPFP pump map. In this case the maps incorporate the friction term as well.

According to the RL00001 document [22] the pump map, Γ_{FP}, accepts a nondimensional flow variable input ϕ and outputs a corresponding nondimensional head variable ψ. The pump map is defined by $\psi_{FP} := \Gamma_{FP}(\phi_{FP})$. The ϕ variable is a function of the pump fuel flow, $D\tilde{W}_{FP}$, density, and pump speed, $\tilde{S}_{FP}$. The pump map will be incorporated here in the following manner: first, ϕ is cast in terms of the dimensional variables, $\tilde{A}$, $\tilde{u}$, $\tilde{\rho}$, and $\tilde{S}_{FP}$. Pump speed is introduced as another input to the model. Second, the output of the map, ψ, is redimensionalized in terms of the pressure difference across the pump, density and pump speed. The map input ϕ must be constructed from the flow variables used in Equation 8. Using the definition of the flow variable consistent with [22], we have

$$\tilde{\phi}_{FP} := \frac{D\tilde{W}_{FP}}{\tilde{\rho}_{FP}\tilde{S}_{FP}} = \frac{\tilde{A}\tilde{u}_{FP}}{\tilde{S}_{FP}}.$$

To construct ϕ, the variables $\tilde{A}$ and $\tilde{u}$ must first be redimensionalized from the variables A_1, M_1. As $\tilde{S}_{FP}$ comes as an external input, it can be used directly. Note that consistent with the explicit form of the model developed here, only system inputs are used. The dimensional ϕ is then nondimensionalized for use in the map. The nondimensional output of the map, ψ is dimensionalized in terms of the pressure across the pump, $\Delta\tilde{P}$, density and pump speed

$$\tilde{\psi} = \bar{\psi}\psi \ ,$$

where $\bar{\psi} := \frac{\Delta \bar{P}}{\bar{\rho} \bar{S}_{FP}^2}$. The dimensional pressure rise across the pump is then given by

$$\tilde{P}_1 - \tilde{P}_0 = \bar{\psi} \tilde{\rho}_0 \tilde{S}_{FP}^2 \ .$$

By inspection of Equation 10 and the equation above, it is seen that after nondimensionalizing the above equation f_2 may be obtained directly as

$$f_2 = \bar{\psi} \psi \ \kappa e^{(P_0 - T_0)} \ \bar{S}_{FP} \tilde{S}_{FP}^2 \ .$$

Some additional steady state experiments where input and output temperatures are measured must be carried out in order to obtain f_3. After constructing f_3 the fact that at steady state the mass flow at the input must equal the mass flow at the output is used to relate f_1 to f_2 and f_3. Thus, one additional map f_3 must be found to complete the nominal model of the SSME HPFP.

Although it seems that more steady state information is needed to actually complete the HPFP nominal model compared to existing models, we now show that the model developed here is the general case while existing models employ some additional assumptions. Indeed, recall that no initial assumptions regarding compressibility or friction were made for the models developed here. Now, suppose that incompressible isentropic flow is assumed. In this case there is no friction or heat transfer so that f_w and Q are zero. The energy equation in steady state then reduces to

$$\frac{d\tilde{T}}{d\tilde{x}} = 0 \ .$$

From Equation 10 it is seen that $f_3 = 0$. If there is no area change then the incompressible continuity equation implies that

$$\frac{d\tilde{u}}{d\tilde{x}} = 0 \ ,$$

which in turn in steady state and nondimensional variables implies that

$$M_1 - M_0 = 0 \ .$$

Consequently, f_1 from Equation 10 drops out as well. Therefore, under incompressible isentropic constant area flow conditions, only one map f_2 need be found to determine the unknown forcing. The RTM, DTM and MARSYAS models consider the flow through the HPFP as incompressible and adiabatic. In light of the above first principles analysis, it would seem that additional assumptions of isentropic flow and no area change were applied as well. However, any SSME schematic where various pressure, flows and temperatures are noted at different points at some rated power level, shows that in fact there are temperature rises in the ducts leading to and from the HPFP. Most likely, there is a temperature rise across the pump as well. Yet, no equations characterizing change in temperature are given in the RTM for liquid flow. Temperature enters the calculations only when gaseous flows are assumed. Even if the temperature rises were lumped in the ducts surrounding the HPFP, the model does not provide a means of calculating these temperature changes. Apparently there exists the following inconsistency. If incompressible and adiabatic conditions prevail then the pump map accounts for both shaft force and friction. However, a means to account for the temperature rise due to the friction is not provided. If incompressible and isentropic conditions prevail then the pump map accounts solely for the shaft force and from the isentropic assumption, the inlet to outlet temperature change should be zero. However, as mentioned above, a rise in temperature is known to exist.

So it is seen that under the assumptions of incompressible and isentropic flow, the steady state maps used in models such as the RTM, are sufficient to complete the nominal HPFP model

developed here. In other words, models like the RTM can be viewed as special cases of the more general model with respect to the assumptions made for the forcing functions.

We consider now the validity of the incompressible assumption made in the RTM and MARSYAS HPFP models. Taking pressures and temperatures from a 109% RPL SSME schematic at approximately the inlet and outlet of the HPFP, and the steady state flow through the HPFP from the RL00001 document, some rough Mach number and density calculations can be made. The schematic used is shown in Figure 5. The density and speed of sound are calculated using the EOS developed in this work. A 17% decrease in Mach number from inlet to outlet is observed. Moreover, calculations show roughly a *45% increase* in density from inlet to outlet. By most engineering standards such a large gradient must be taken into account. According to [3], only density changes of not more than 5% warrant the incompressibility assumption. Although the Mach numbers are low $\sim .05$, it must be remembered that the substance is a *liquid*, not a gas, so that the standard practice in gas dynamics of equating low Mach numbers with incompressibility no longer applies. In many situations, liquids can be considered to be incompressible because they are not subjected to extreme pressures. In the case of waterhammer, however, where pressure quickly rises proportionally to the speed of sound [21, 9, 26], compressibility effects are considered. Similarly, in the case of the HPFP, LH_2 undergoes a tremendous pressure increase as it flows through the HPFP. From this analogy, assuming most liquids exhibit similar thermodynamic and fluid dynamic behavior, a considerable change in density is to be expected. It seems that the more general case which includes compressibility effects should be used to account for the temperature rise and density change seen across the SSME HPFP.

In addition to lack of temperature input/output information, other problems concerning geometric parameters and model comparison were encountered. For $\bar{L}$, the length of the pump, care must be taken to account for the helical path the fluid follows as it flows through pump. This can be accomplished provided that the axial pump length is known. The correct inlet and outlet areas must also be obtained. Because of the rigorous first principles based modelling method that utilizes no extra correction factors, it is crucial to obtain the actual lengths and areas in order to match both steady state and dynamic HPFP behavior. Unfortunately, attempts to glean geometry information from the RTM, DTM and MARSYAS models have failed as the information is buried so deeply or combined with other parameters that extraction of the necessary lengths and areas is impossible. Once a working model is up and running, it will be difficult to compare to the DTM HPFP model because it is unclear how to isolate the HPFP component. Again, this is a reflection of the rather vague component boundaries typical of the DTM.

The next section discusses how certain anomalous conditions can be modelled using the uncertainty and signal representations mentioned in Section 1.

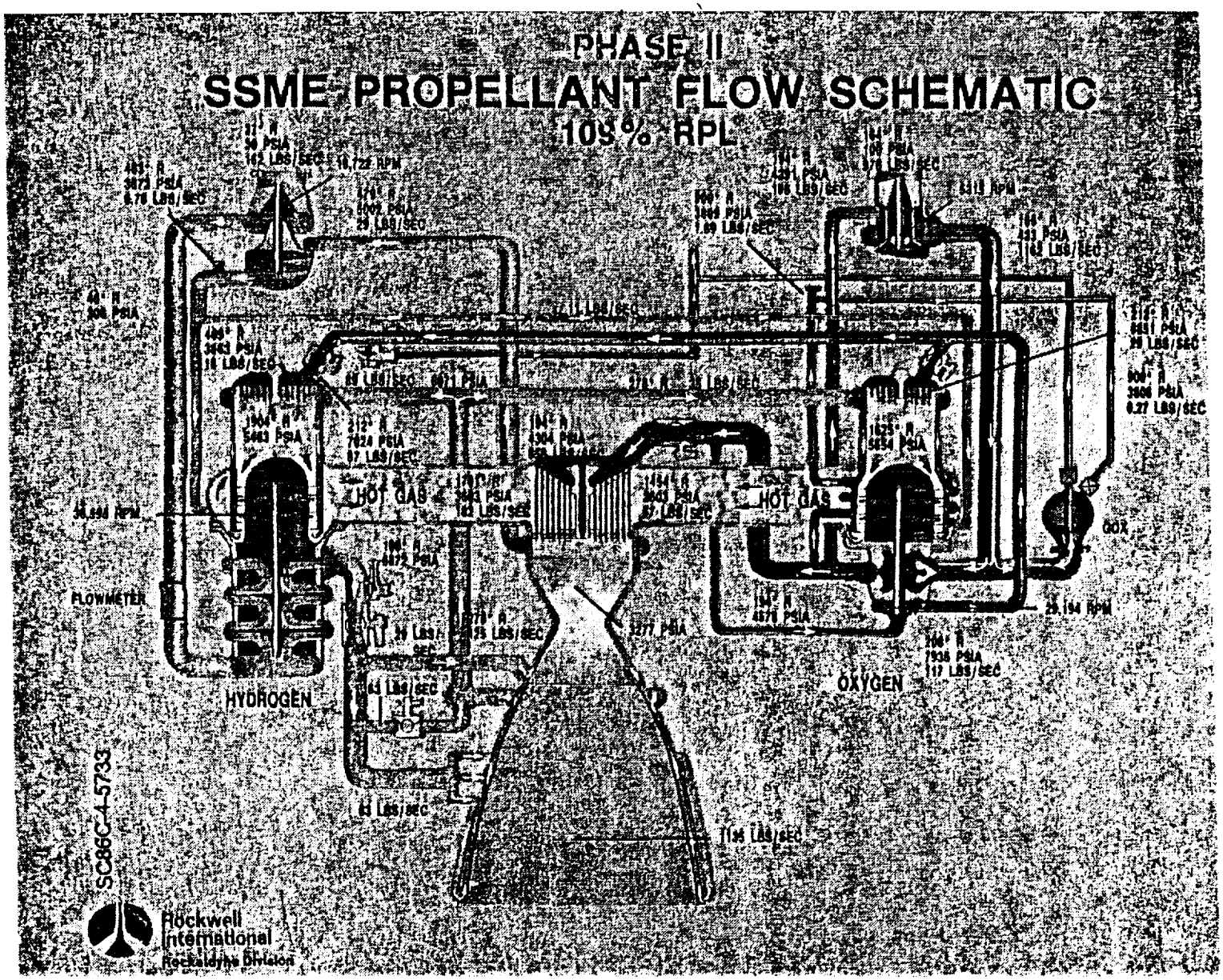

Figure 5: Schematic of SSME at 109% RPL

ORIGINAL PAGE IS
OF POOR QUALITY

12 SSME HPFP Anomalous Model

In order to apply model based condition monitoring, there must exist a way to incorporate anomalous conditions into the system model. As pointed out in Section 1.1, the empirical approach to model development may not yield a model capable of matching anomalous hot fire test data. Such models need "tuning" via special "corrective factors" to match nominal hot fire test data. A model tuned to reflect nominal conditions becomes "out of tune" to anomalous conditions. Typically, the "corrective factors" are an amalgamation of individual system properties Once formed, however, it is difficult extricate the original properties from the factors so that the factors have no physical meaning. Consequently, in tweeting the factors to match steady state, there is no way of discerning which physical properties are changing.

The control and condition monitoring based approach allows nominal models to be augmented, in a rigorous manner, with portions describing anomalous behavior. The signal and uncertainty representations of anomalous conditions introduced in Section 1 are applied here to the HPFP.

Signal representation involves the injection of an extraneous signal at the system input or output characterizing the anomaly. Figure 6 illustrates signal representation of anomalous conditions. Injecting a signal of zero magnitude reflects nominal behavior.

Uncertainty representation treats anomalous conditions as a dynamic block multiplicatively or additively augmented to the nominal model. Figure 7 depicts the three ways the delta block can be augmented to the nominal model. The delta block contains dynamic representations of anomalous conditions and reflects the uncertainty about the system behavior introduced by the anomalies. A zero value for delta reduces to the nominal model. The choice of scheme depends on the type of anomalous condition. If an anomaly has some dynamics associated with it, then the uncertainty representation is appropriate. If the anomaly manifests itself as an extraneous signal independent of the inputs, then the signal representation is applicable. The basic approach of the two schemes is illustrated below in Sections 12.1 and 12.2 by two specific cases of HPFP failure modes taken from SSME failure documentation [1].

Figure 6: Signal Representation

12.1 Pump Speed Disturbance

Consider a disturbance, δS_{FP}, in the pump speed, S_{FP}, so that the actual input to the pump becomes

$$S_{FP} = \hat{S}_{FP} + \delta S_{FP} \ ,$$

where $\hat{S}_{FP}$ is the nominal speed. As the disturbance is assumed independent of the input nominal speed, it is seen that δS_{FP} can be modelled as a signal injected at the input to the nominal model as shown in the left part of Figure 6. Note that $\hat{S}_{FP}$ appears as one of the external inputs to the steady state map, f_2.

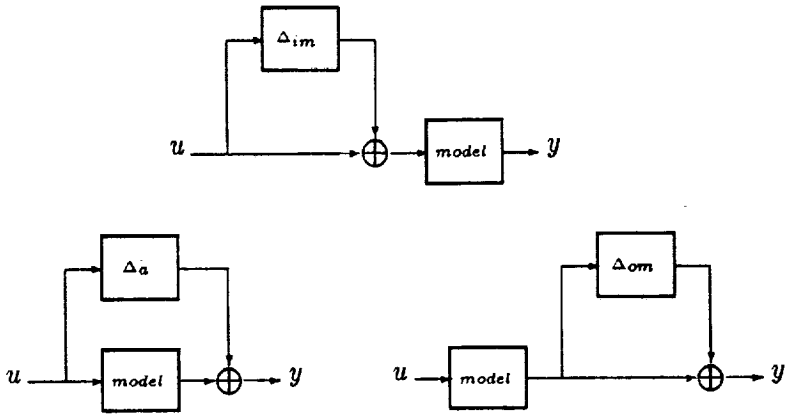

Figure 7: Uncertainty Representation

12.2 Fuel Leak

Fuel leaks caused by seal degradation can lead to problems as serious as complete engine failure. Consider a damaged seal at the input volute that establishes another flow path through the leak. The region around this leak becomes another element in the model. The dimensional inputs to this element consist of the inlet volute pressure just upstream from the leak, $\tilde{P}_0$, the inlet volute temperature just upstream of the leak, $\tilde{T}_0$, and the inlet flow, $D\tilde{W}_0$. The outputs include the pressure across the inlet volute, $\tilde{P}_{do}$, the pressure across the leak, $\tilde{P}_{lk}$, the temperature at the inlet volute, $\tilde{T}_{do}$, the temperature across the leak, $\tilde{T}_{lk}$, the flow through the leak, $D\tilde{W}_{lk}$, and the flow just downstream of the inlet, $D\tilde{W}_{do}$.

As the split in the flow occurs over a very short axial distance, the dynamics of this component can be residualized. Furthermore, it is assumed that the fluid properties (pressure and temperature) just upstream of the leak are equal to the fluid properties at the inlet volute. Since temperatures and pressures are the same then it follows that the densities should also be the same. From these assumptions the following equations hold:

$$D\tilde{W}_0 = D\tilde{W}_{do} + D\tilde{W}_{lk}$$

or by expanding the flow terms,

$$\begin{aligned}
\tilde{\rho}_0\tilde{A}_0\tilde{u}_0 &= \tilde{\rho}_{do}\tilde{A}_{do}\tilde{u}_{do} + \tilde{\rho}_{lk}\tilde{A}_{lk}\tilde{u}_{lk} \\
\tilde{P}_0 &= \tilde{P}_{do} = \tilde{P}_{lk} \\
\tilde{T}_0 &= \tilde{T}_{do} = \tilde{T}_{lk} \\
\tilde{\rho}_0 &= \tilde{\rho}_{do} = \tilde{\rho}_{lk} \\
\tilde{A}_0 &= \tilde{A}_{do} \, .
\end{aligned}$$

Because the leak can be treated as an orifice, the well-known orifice equation [21]

$$\tilde{u}_{lk} = c_{d1}\sqrt{\frac{2}{\tilde{\rho}_0}(\tilde{P}_0 - \tilde{P}_a)} \tag{11}$$

applies. The dimensionless orifice coefficient is defined as

$$c_{d1} := \frac{1}{\sqrt{1 - \frac{c_c\tilde{A}_{lk}}{\tilde{A}_0}^2}}$$

where c_c is the contraction coefficient which depends on the type of orifice. Here we assume a sharp edged orifice. In this case, c_c is taken from [33] to be $c_c = .62$. The pressure, $\tilde{P}_a$, is the ambient pressure present on the other side of the leak. Simplifying the above continuity equation yields

$$\tilde{u}_0 = \tilde{u}_{do} + \tilde{u}_{lk}\frac{\tilde{A}_{lk}}{\tilde{A}_0} .$$

Substituting the orifice Equation 11 into this equation, nondimensionalizing and simplifying we have

$$M_0 = M_{do} + c_d\sqrt{2(P_0 - P_a)} \tag{12}$$

where

$$c_d := c_{d1}\frac{A_{lk}}{A_0} .$$

In order to use Equation 12 in conjunction with the nominal model, the derivative with respect to time must be taken and the result substituted in for M_0. The most general case includes both a time varying leak area, imbedded in the discharge coefficient c_d, and time varying input pressure, P_0. The time derivative of Equation 12 is given below

$$\frac{d}{dt}M_{do} = \frac{d}{dt}M_0 - \frac{c_d}{\sqrt{2(P_0 - P_a)}}\frac{d}{dt}P_0 - \frac{c_{d1}}{A_0}(c_c{}^2 c_{d1} c_d + 1)\sqrt{2(P_0 - P_a)}\,\frac{d}{dt}A_{lk} \tag{13}$$

To complete the leaky model, Equation 13 is augmented to the nominal model by an additional dynamic block consisting of

$$\Delta_a = \frac{c_d}{\sqrt{2(P_0 - P_a)}}\frac{d}{dt}P_0 + \frac{c_{d1}}{A_0}(c_c{}^2 c_{d1} c_d + 1)\sqrt{2(P_0 - P_a)}\,\frac{d}{dt}A_{lk} .$$

Note that the Mach number associated with the leak is given by $M_{lk} = c_d\sqrt{2(P_0 - P_a)}$. Substituting this relation into the Δ equation yields

$$\Delta_a = \frac{c^2{}_d}{M_{lk}}\frac{d}{dt}P_0 + \frac{c_{d1}}{A_0 c_d}(c_c{}^2 c_{d1} c_d + 1)M_{lk}\,\frac{d}{dt}A_{lk} . \tag{14}$$

This anomalous behavior is modelled using the uncertainty representation.

The fundamental parameter determining the amount of uncertainty is based upon the size of the leak area, A_{lk}. When the leak area is zero, $c_d \to 0$ and the anomalous block, Δ_a, reduces to zero restoring the nominal model. The above two examples illustrate how anomalous conditions can be modelled as additional portions augmented to the nominal model. The complete anomalous model becomes the aggregate of the anomalous portion and the nominal portion.

13 Conclusions

This work presents a rigorous liquid propulsion modelling method for condition monitoring and control. Some key attributes of this method are the following:

1. Thermodynamic and fluid dynamic properties for a liquid such as LH_2 are incorporated into the governing conservation dynamic equations via a novel equation of state.

2. Information from steady state input/output experiments can be folded into the model in a straight forward manner, as dictated by the equations, to determine unknown terms such as friction or heat transfer effects. Vague correction terms are not used to match actual steady state behavior.

3. A nondimensionalization procedure frees the equations form a particular set of units and transforms them into a more elegant form. Moreover, the procedure introduces a dimensionless parameter that can be used to reduce model dynamic order.

4. Via a discretization and state assignment method, lumped parameter components are obtained that exploit the system's natural boundaries.

5. Anomalous conditions are modelled by augmenting the nominal model with a dynamic uncertainty block representation or an extraneous signal representation of anomalous conditions. The anomalous model is an aggregate of the nominal portion and the portion reflecting anomalous behavior. The nominal model remains unaltered and can be easily recovered from the aggregate anomalous model by allowing the anomalous portion to vanish.

This method is deemed condition monitoring and control oriented as it can generate models that are reduced order and that can describe anomalous conditions. The former is desired for control while the latter is needed for condition monitoring.

Preliminary results involving the SSME HPFP imply that models developed using this approach are especially suited for liquid rocket engine systems provided that system geometry and certain static input/output relationships can be acquired. Given the wealth of data available for the SSME, this does not seem unattainable. Discussions with experts in the at MSFC alerted the authors to some practical considerations concerning model validation. For one, the coupling effects between adjacent components of the SSME make it difficult to test individual components developed here against similar components from the DTM. In order to exploit information from the DTM model, a model of at least one side, i.e. fuel, of the SSME should be built following the method herein and then compared to the DTM. As system model order reduction using the ϵ parameter should really be done after the entire system is complete, this would actually be more faithful to the modelling approach developed here. Another consideration is the effect that the various assumptions regarding flow conditions and forcing terms have on the existing models as compared to the model developed here. In Section 11 it was seen that under the additional assumptions of incompressibility and isentropic flow, the forcing function of the nominal model could be determined by steady state information from the RTM. However, it is not entirely clear what assumptions beyond incompressible flow were made for models like the RTM. If an additional isentropic assumption is included, then the model fidelity to the real system is sacrificed since a temperature rise does occur across the actual HPFP. If friction is included then the temperature rise, now allowed by first principles considerations, is not accounted for by the model. Moreover, it was found that the approximate density change across the HPFP is well above the standard change allowable for the incompressible flow assumption.

Although the existing models are themselves based on first principles, approximations and assumptions employed because of practical considerations, especially the correction factors, have made the models rather cumbersome and incomplete. They are cumbersome because of complex component interconnections and high model order. Individual components such as the HPFP cannot be easily extracted from the whole model in order to compare it with other models of the HPFP. The DTM has about 200 states which makes it very difficult to use in conjunction with a sophisticated controller. They are incomplete because not all flow variables are always available for all components, for example the HPFP outlet temperature in the RTM model.

The approach developed here employs a sequence of steps where all assumptions and approximations are clearly defined and first principles are followed as much as possible. When it becomes necessary to resort to steady state experiments, that information is incorporated in a rigorous manner. The model equations clearly indicate which parts are from first principles and which parts are steady state maps. The nondimensionalization procedure yields ϵ parameters for each component whereupon their *relative* magnitudes determine which component dynamics, if any, can be residualized. Since the nondimensional equations are independent of units the problem of comparing the dynamics of a continuity equation in terms of density to one in terms of pressure is alleviated. Through the discretization and state assignment process, model components have distinct boundaries and thus clearly defined inputs/outputs. This modular concept should greatly facilitate model analysis and simulation, for example the nominal HPFP model could be easily replaced by an anomalous one without having to change the other SSME model components. Control and condition based modelling is seen not only as an improvement over existing modelling methods in developing models for integrated control and condition monitoring systems but also as a well structured, consistent modelling tool in general.

References

[1] SSME failure modes and effects analysis and critical items. Technical report, Rockwell International, Rocketdyne Division, may 1986.

[2] Y. Adachi and H. Sugie. Effect of substance-dependent Ω_{ac} on vapor-liquid equilibrium calculations. *The Canadian Journal of Chemical Engineering*, 63:490–496, June 1985.

[3] J. Anderson. *Introduction to Flight.* McGraw-Hill Book Co., 3rd edition, 1989.

[4] J. Anderson. *Modern Compressible Flow.* McGraw-Hill, 1990.

[5] O. Badmus, S. Chowdhury, K. Everker, and C. Nett. Control-oriented high-frequency turbomachinery modeling: Single-stage compression system 1D model. In *ASME International Gas Turbine and Aeroengine Congress and Exposition*, 1993. ASME 93-GT-385.

[6] O. Badmus, K. Eveker, and C. Nett. Control-oriented high-frequency turbomachinery modeling: General 1D model development. In *ASME International Gas Turbine and Aeroengine Congress and Exposition*, 1993. ASME 93-GT-18.

[7] O. Badmus, K. Eveker, and C. Nett. Control-oriented high-frequency turbomachinery modeling: Theoretical foundations. In *1992 Joint Propulsion Conference*, 1993. AIAA paper no. 92-3314.

[8] J. Bentsman, M. Wilcutts, and A. Pearlstein. Control oriented modeling of combustion and flow processes in liquid propellant rocket engines. *AIAA*, July 1990.

[9] M. Chaudry. *Applied Hydraulic Transients.* Van Norstrand Reinhold Co., 1979.

[10] J. Dufour and W. Nelson. *Centrifugal Pump Sourcebook.* McGraw-Hill, Inc., 1993.

[11] V. Faires and C. Simmang. *Thermodynamics.* Macmillan Publishing Co., 1978.

[12] A. Harmens and D. Jeremiah. On two-parameter equations of state and the limitations of a hard sphere Peng-Robinson equation. *Cryogenics*, 25:60–62, February 1985.

[13] A. Helmicki, S. Jaweed, and K. Kolcio. An integrated approach to rocket conditon monitoring and control. In *Fourth Annual Space System Health Management Technology Conference*, November 1992.

[14] A. Helmicki, F. Kuo, and D. Vallely. Rocket engine health monitoring and control: Some connections and their implications. In *Proceedings 3rd Annual Health Monitoring Conf. for Space Propulsion Systems*, Cincinnati, Ohio, November 1991.

[15] A. J. Helmicki. Rocket engine health monitoring: A system's perspective. TechnicalReport, NASA Marshall Space Flight Center, August 1991.

[16] R. Isermann. Process fault detection based on modeling and estimation methods: A survey. *Automatica*, 20(4):387–414, July 1984.

[17] J. J. Lienhard, N. Shamsundar, and P. O. Biney. Spinodal lines and equations of state: a review. *Nuclear Engineering and Design*, 95:297–314, August 1986.

[18] C. Lin and L. Segel. *Mathematics Applied to Deterministic Problems in the Natural Sciences.* Macmillan Publishing Co., 1974.

[19] L. G. Loitsyanskii. *Mechanics of Liquids and Gases.* Pergamon Press, 1966.

[20] R. McCarty. *Hydrogen: Its Technology and Implications: Hydrogen Properties*, volume 3. CRC Press, 1975.

[21] H. Merritt. *Hydraulic Control Systems.* John Wiley and Sons, 1967.

[22] D. Nguyen. Engine balance and dynamic model. Technical report, Rockwell International, Rocketdyne Division, Canoga Pk., Ca, 1981.

[23] A. Norman, I. Cannon, and L. Asch. The history and future of safety monitoring in liquid rocket engines, 1989.

[24] A. Norman and M. Taniguchi. Development of an advanced failure detection algorithm for the SSME. In *Proc. AIAA/SAE/ASME/ASEE 29th Joint Propulsion Conference*, Boston, Mass, July 1988. AIAA paper no 88-3408.

[25] H. Panossian, V. Kemp, R. Nelson, and M. Taniguchi. Real-time fault detection algorithm for the Space Shuttle Main Engine. AIAA publication.

[26] J. Parmakian. *Waterhammer Analysis.* Prentice Hall, 1955.

[27] K. Shah and G. Thodos. A comparison of equations of state. *Industrial and Engineering Chemistry*, 57(3):30–37, March 1965.

[28] W. Sheng and B.-Y. Lu. Quantum correction of cubic equation of state for fluids at cryogenic conditions. *Advances in Cryogenic Engineering*, 35:1503–1510, 1990.

[29] E. Taylor. *Dimensional Analysis for Engineers.* Oxford University Press, 1974.

[30] J. Tiller. MARSYAS SSME model. Technical report, BCSS, MSFC, Huntsville, Al, 1991.

[31] D. Tritton. *Physical Fluid Dynamics.* Oxford University Press, 1988.

[32] R. Turton. *Principles of Turbomachinery.* E. & F.N. Spon, 1984.

[33] J. Vennard and R. Street. *Elementary Fluid Mechanics.* John Wiley and Sons, 1976.

[34] S. Wolfram. *Mathematica, A System for Doing Mathematics by Computer.* Addison-Wesley, 1988.